

# [UF<sub>6</sub>]<sub>2</sub><sup>-</sup>: A Molecular Hexafluorido Actinide(IV) Complex with Compensating Spin and Orbital Magnetic Moments

Kasper S. Pedersen,\* Katie R. Meihaus, Andrei Rogalev,\* Fabrice Wilhelm, Daniel Aravena, Martín Amoza, Eliseo Ruiz, Jeffrey R. Long, Jesper Bendix, and Rodolphe Clérac\*

**Abstract:** The first structurally characterized hexafluorido complex of a tetravalent actinide ion, the [UF<sub>6</sub>]<sub>2</sub><sup>-</sup> anion, is reported in the (NEt<sub>4</sub>)<sub>2</sub>[UF<sub>6</sub>]<sub>2</sub>·2H<sub>2</sub>O salt (**1**). The weak magnetic response of **1** results from both U(IV) spin and orbital contributions, as established by combining X-ray magnetic circular dichroism (XMCD) spectroscopy and bulk magnetization measurements. The spin and orbital moments are virtually identical in magnitude, but opposite in sign, resulting in an almost perfect cancellation, which is corroborated by *ab initio* calculations. This work constitutes the first experimental demonstration of a seemingly non-magnetic molecular actinide complex carrying sizable spin and orbital magnetic moments.

The chemistry of uranium compounds and the diversity of potential uses for uranium in novel materials are currently experiencing a renaissance.<sup>[1]</sup> Molecular complexes with uranium in either +III or +V oxidation states have been shown to generally exhibit slow relaxation of magnetization,<sup>[2]</sup> together with a single U(IV) complex that appears as an exception.<sup>[3]</sup> Such complexes are also interesting building-blocks for magnetic polynuclear

complexes and one-dimensional coordination polymers.<sup>[4]</sup> Recent spectroscopic investigations have aimed at a detailed understanding of the electronic structure of actinide ions, which is significantly more complicated than for lanthanides.<sup>[5]</sup> The large spin-orbit coupling of actinide ions and the less shielded nature of their 5f orbitals relative to the 4f orbitals, result in much stronger interactions of the f-electrons with the surrounding atoms. Hence, the concomitant stronger ligand field cannot be considered as a perturbation, particularly for the early members of the 5f series. Furthermore, spectroscopic data of actinide systems are typically very rich and the determination of the electronic energy level-splitting and -composition remains quite challenging. For the magnetic characterization of actinide-based materials, powder and thermodynamically averaged magnetization data bring only limited information about the underlying physics. However, since the magnetic properties are predominantly defined by the energy levels that are thermally populated at room temperature and below, any additional experimental information on these low-lying energy levels would be of great relevance. For this task, X-ray magnetic circular dichroism spectroscopy is a powerful tool able to deconvolute the macroscopically measured magnetic moment into its spin and orbital contributions.<sup>[6]</sup> Despite its routine applications in magnetism, this technique has never been applied to molecular actinide systems.<sup>[7]</sup> Inspired by the early works of Ryan *et al.* and Brown *et al.*,<sup>[8a,8b]</sup> we herein report the synthesis and crystal structure of (NEt<sub>4</sub>)<sub>2</sub>[UF<sub>6</sub>]<sub>2</sub>·2H<sub>2</sub>O (**1**) featuring the first structurally characterized example of an octahedral fluoride complex in the tetravalent actinide family.<sup>[8]</sup> This molecular entity combines a high symmetry coordination sphere with the redox-inactive nature of the predominantly ionic U–F bonds that, supposedly, would facilitate the comparison of the experimental results with theoretical calculations on an isolated U<sup>4+</sup> ion. Although the octahedral complexes [UF<sub>6</sub>] and [UF<sub>6</sub>]<sup>-</sup> are well-described and have been structurally characterized,<sup>[9]</sup> the existence of an octahedral [UF<sub>6</sub>]<sub>2</sub><sup>-</sup> has only been inferred from vi-

- [\*] Assist. Prof. Dr. K. S. Pedersen, Dr. Hab. R. Clérac  
CNRS, CRPP, UMR 5031, F-33600 Pessac (France)  
E-mail: [clerac@crpp-bordeaux.cnrs.fr](mailto:clerac@crpp-bordeaux.cnrs.fr)
- Assist. Prof. Dr. K. S. Pedersen, Dr. Hab. R. Clérac  
Univ. Bordeaux, CRPP, UMR 5031, F-33600 Pessac (France).
- Assist. Prof. Dr. K. S. Pedersen  
Department of Chemistry, Technical University of Denmark, DK-2800 Kgs. Lyngby (Denmark).  
E-mail: [kastp@kemi.dtu.dk](mailto:kastp@kemi.dtu.dk)
- Dr. K. Meihaus, Prof. Dr. J. R. Long  
Department of Chemistry, University of California, Berkeley, California 94720 (USA).
- Dr. A. Rogalev, Dr. F. Wilhelm  
European Synchrotron Radiation Facility, BP 220, 38043 Grenoble Cedex 9 (France).  
E-mail: [rogalev@esrf.fr](mailto:rogalev@esrf.fr)
- Dr. D. Aravena  
Departamento de Química de los Materiales, Facultad de Química y Biología, Universidad de Santiago de Chile (USACH), Casilla 40, Correo 33, Santiago (Chile).
- M. Amoza, Prof. Dr. E. Ruiz  
Departament de Química Inorgànica i Orgànica and Institut de Química Teòrica i Computacional, Universitat de Barcelona, Diagonal 645, 08028 Barcelona (Spain).
- Prof. Dr. J. R. Long  
Materials Sciences Division, Lawrence Berkeley National Laboratory, Berkeley, California 94720 (USA).
- Prof. Dr. J. R. Long  
Department of Chemical and Biomolecular Engineering, University of California Berkeley, Berkeley, California 94720 (USA).
- Prof. Dr. J. Bendix  
Department of Chemistry, University of Copenhagen, DK-2100 Copenhagen (Denmark).
- Supporting information and the ORCID identification number(s) for the author(s) of this article can be found under:  
<https://doi.org/10.1002/anie.xxxxx>

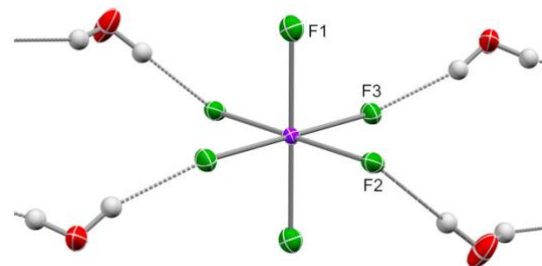


**Figure 1.** Molecular structure of the [UF<sub>6</sub>]<sub>2</sub><sup>-</sup> complex in **1** (thermal ellipsoids drawn at 50% probability level) and the hydrogen bonding pattern linking [UF<sub>6</sub>]<sub>2</sub><sup>-</sup> complexes into supramolecular chains running along the crystallographic *c* direction (see Supporting Information, Figure S1). Selected bond lengths (Å) and angles (°): U–F1 2.124(2), U–F2 2.177(2), U–F3 2.181(2), ∠*cis*-F–U–F 89.23(7)–90.90(7). Color codes: U, purple; F, green; O, red; C, black; H, grey.

brational spectroscopy, but not confirmed by X-ray crystallography.<sup>[8a,8b]</sup> Indeed, more generally, despite the vast number of known fluoride complexes of the actinide ions in oxidation state +IV, none of the hexafluoride complexes have been structurally characterized.

The reaction of  $\text{UF}_4 \cdot x\text{H}_2\text{O}$  ( $x \approx 1.5$ ) with  $\text{NEt}_4\text{F} \cdot \text{H}_2\text{O}$  in propylene carbonate under a dry  $\text{N}_2$  atmosphere yields a pale green solution. Addition of acetone induces the crystallization of a pale-green material suitable for single-crystal X-ray diffraction. The crystal structure analysis of  $(\text{NEt}_4)_2[\text{UF}_6] \cdot 2\text{H}_2\text{O}$  (**1**) reveals the presence of slightly compressed octahedral  $[\text{UF}_6]^{2-}$  complexes (Figure 1), with U–F bond lengths being longer for fluoride ligands engaged in hydrogen bonding (2.177(2) and 2.181(2) Å versus 2.124(2) Å; Figure S1). The U–F bond lengths are also significantly longer than those found in  $[\text{UF}_6]^-$  (av. U–F 2.03 Å) and  $[\text{UF}_6]$  (av. U–F 1.98 Å),<sup>[10]</sup> but comparable to those of organometallic U(IV) complexes such as  $[\text{Cp}^*\text{zUF}_2(\text{py})]$  ( $\text{Cp}^*$  = pentamethylcyclopentadienide, py = pyridine; av. U–F 2.15 Å) and  $[\text{Cp}_3\text{UF}]$  ( $\text{Cp}$  = cyclopentadienide; U–F 2.11 Å).<sup>[11]</sup>

The temperature dependence of the magnetic susceptibility-temperature product,  $\chi T$ , of **1** is shown in Figure 2a. From 0.35  $\text{cm}^3 \text{K mol}^{-1}$  at 300 K, it nearly vanishes to  $5 \times 10^{-3} \text{ cm}^3 \text{K mol}^{-1}$  at 1.8 K, which is far from the 1.60  $\text{cm}^3 \text{K mol}^{-1}$  value expected for the Russell-Saunders atomic ground state term of the  $5f^2$  configuration ( $3H_4$ ,  $g_J = 4/5$ ).<sup>[12]</sup> The  $\chi T$  value at 300 K is consistent with temperature independent paramagnetism due to interaction with low energy excited states. In order to obtain experimental information on the nature of the electronic ground state of uranium in **1**, X-ray absorption spectroscopy (XAS) and X-ray magnetic circular dichroism (XMCD) were employed. The spectra of **1** at the uranium  $M_{4,5}$  absorption edges were obtained at the ID12 beamline (European Synchrotron Radiation Facility, ESRF) in large magnetic fields of up to 17 T at 4 K. Since the experiments were performed on polycrystalline samples, the isotropic XAS spectra were approximated from  $(\sigma^+ + \sigma^-)/2$ , whereas XMCD spectra are given by the spectral  $(\sigma^+ - \sigma^-)$  difference. Here,  $\sigma^+$  ( $\sigma^-$ ) is the absorption cross-section obtained with helicity and magnetization aligned either parallel (+) or antiparallel (–). The  $M_{4,5}$  XAS spectra are dominated by strong resonance lines, so-called “white lines”, due to dipole-allowed transitions from the

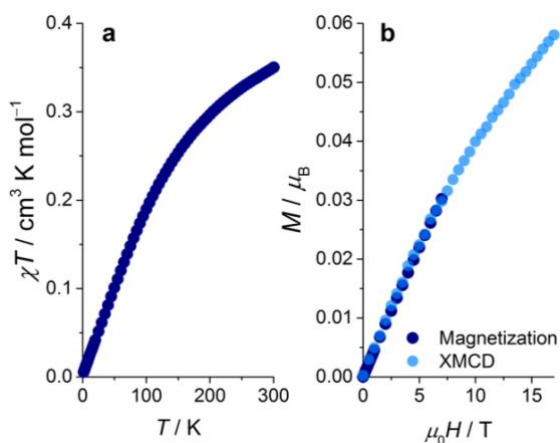


**Figure 2.** (a) Temperature dependence of the  $\chi T$  product ( $\chi$  being the magnetic susceptibility defined as  $M/\mu_0 H$ ) over the 1.8–300 K range (0.3 K  $\text{min}^{-1}$ ) of a polycrystalline sample of **1** obtained with  $\mu_0 H = 1.0$  T. (b) Field-dependence of the magnetization,  $M(\mu_0 H)$ , obtained at 4 K in the 0–7 T range and the scaled field dependence of the XMCD signal measured in the 0–17 T range at a photon energy of 3727.3 eV corresponding to the maximum of the XMCD signal at the  $M_4$  edge.

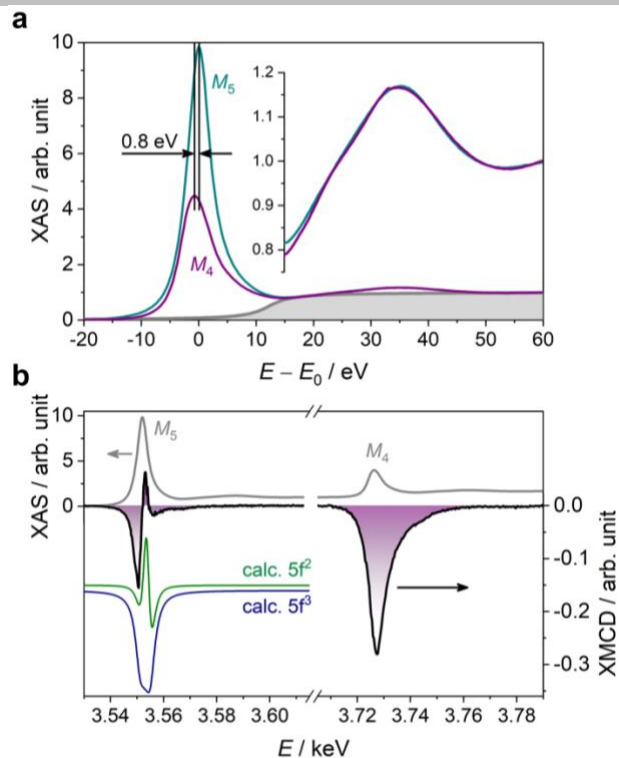


**Figure 3.** (a) Isotropic XAS spectra of **1** obtained at the  $M_5$  and  $M_4$  edges shown on the same relative energy scale (see Supporting Information). The gray line represents the step function used for spectra integration. The inset is a magnification of the first EXAFS oscillation used to build the relative energy scale. (b) XMCD spectra of **1** (black lines) obtained at the  $M_5$  and  $M_4$  edges in a magnetic field of  $\mu_0 H = 17$  T at  $T = 4$  K. The filled patterns indicate the integrals employed for the magneto-optical sum rules analysis. The theoretical XMCD spectra for both the  $5f_2$  (green trace) and  $5f_3$  (navy trace) configurations were obtained from multiplet calculations employing the ligand field parameters extracted from *ab initio* calculations (*vide infra*, Figures S2 & S3).

spin-orbit split  $3d_{3/2,5/2}$  levels into the magnetic  $5f$  states along with much weaker  $3d \rightarrow 6p$  and  $3d \rightarrow$  continuum transitions. According to the dipole selection rule ( $\Delta j = \pm 1$ ), the larger  $M_5$  white line intensity primarily reflects the population of the  $5f_{7/2}$  states and the weaker  $M_4$  intensity only the  $5f_{5/2}$  states.<sup>[13]</sup> In Figure 3a, the XAS spectra  $M_{4,5}$  are shown on the same relative energy scale that is obtained by shifting the original spectra (Figure 3b, gray trace) in order to perfectly overlap the first EXAFS oscillation (inset Figure 3a). It is apparent, that the absorption maxima of the  $M_5$  and  $M_4$  white lines are at different photon energies separated by  $\sim 0.8$  eV with the  $M_4$  peak being at lower photon energies. This energy splitting is due to spin-orbit coupling of the  $5f$  states. In a spherically symmetric ligand field, the magnitude of this gap can be approximated by  $\Delta E = 7/2 \zeta_{5f}$ , where  $\zeta_{5f}$  is the spin-orbit parameter for the  $5f$  electrons. The angular part of the spin-orbit interaction for the  $5f$  states,  $\langle \sum \mathbf{l}_i \cdot \mathbf{s}_i \rangle$ , can be obtained using the so-called spin-orbit sum rule which relates its ground state expectation value to the branching ratio of the isotropic X-ray absorption intensities.<sup>[14]</sup> For uranium  $M_{4,5}$  edges, one obtains  $2\langle \sum \mathbf{l}_i \cdot \mathbf{s}_i \rangle / 3n_{5f} \approx -5/2[\text{BR} - 3/5]$ , where BR is given by  $I_{M_5}/(I_{M_5} + I_{M_4})$  (“ $I$ ” indicates the integral over a white line) and  $n_{5f}$  is the number of holes in the  $5f$  levels.<sup>[15]</sup> For essentially ionic complexes such as  $[\text{UF}_6]^{2-}$ , the number of holes in the  $5f$  levels amounts to  $n_{5f} = 12$ . The experimental value of  $\text{BR} = 0.727 \pm 0.005$  of **1** results in  $\langle \sum \mathbf{l}_i \cdot \mathbf{s}_i \rangle / \hbar^2 \approx -5.7$ , which is significantly larger than the values obtained by atomic calculations on the  $5f_2$  configuration of  $-3$ ,  $-4$ ,

and  $-3.88$  in the Russell-Saunders,  $jj$ , and intermediate coupling scheme, respectively.<sup>[16]</sup> However, it corresponds surprisingly well to the  $jj$  or intermediate coupling scheme values ( $-6$  and  $-5.34$ ) for a  $5f_3$  configuration, which, however, is incompatible with the chemical identity and magnetization data of the present system. One should bear in mind that the spin-orbit sum rule has been derived assuming no hybridization between the core and valence state and neglecting the core-valence interaction. The observed deviation from theory is thus not unexpected because of the highly localized nature of the  $5f$  states in **1**, where core-valence interaction could be very strong. Indeed, such discrepancies with theoretical models have already been observed in electron energy loss spectroscopy results obtained on various U(IV) oxide minerals.<sup>[17]</sup>

The normalized XMCD spectra at the uranium  $M_{4,5}$  edges are shown on [Figure 3b](#). Sizeable dichroism signals are observed at both  $M_4$  and  $M_5$  edges. The spectral shape of the XMCD at the  $M_5$  edge is in very good agreement with the one estimated from multiplet calculations for the  $5f_2$  configuration with a cubic ligand field ([Figure 3b](#), green trace), and with experimental results on U(IV)-containing metals.<sup>[13]</sup> This favorable comparison of uranium  $M_5$  XMCD spectral shape, which is extremely sensitive to the  $5f$  occupation, confirms also the  $5f_2$  configuration of uranium in **1**. To deduce the magnitudes of the magnetic moments carried by the uranium  $5f$  states, one can use the so-called magneto-optical sum rules, which relate the integrals of the XMCD spectra to the orbital (orbital sum rule)<sup>[18]</sup> and spin (spin sum rule)<sup>[19]</sup> magnetic moments. Unfortunately, the spin sum rule is based on the same approximation as the spin-orbit sum rule, and can therefore hardly be applied to our XMCD spectra. Nevertheless, the orbital sum rule remains valid irrespective of this approximation and numerical integration of the XMCD spectra shown in [Figure 3b](#) affords  $M_{\text{orbital}} = 0.47 \mu_B$ . The spin moment,  $M_{\text{spin}}$ , may hereafter be determined by first scaling the magnetization curve measured by monitoring the  $M_4$  XMCD signal as a function of applied magnetic field (shown in [Figure 2b](#)) to the macroscopic magnetization data. This procedure allows the estimation of the absolute magnetization at 17 T, which amounts to only  $M_{\text{total}} = 0.060(4) \mu_B$ , thereby yielding  $M_{\text{spin}} = -0.41 \mu_B$  through the  $M_{\text{total}} = M_{\text{orbital}} + M_{\text{spin}}$  relation. Thus, the analysis of the XMCD spectra reveals, unambiguously, the existence of sizable orbital and spin magnetic moments in **1** despite a low bulk magnetic moment. Similar cancellation of spin and orbital magnetizations for uranium has been already observed in itinerant  $5f$  systems like  $\text{UFe}_2$  using neutron scattering and confirmed by XMCD.<sup>[15]</sup> Here we demonstrate that the spin-orbital cancellation is not limited to metallic systems with strongly delocalized  $5f$  states but is also present in a molecular system with much higher degree of  $5f$  localization.

*Ab initio* CASSCF<sup>[20]</sup> calculations based on the crystallographic geometry of the  $[\text{UF}_6]^{2-}$  complex predict significantly lower orbital and spin magnetic moments of the ground state ( $M_{\text{orbital}} = -0.056 \mu_B$  and  $M_{\text{spin}} = 0.020 \mu_B$ ). The addition of dynamic correlation by the NEVPT2<sup>[21]</sup> method does not significantly modify the CASSCF picture ( $M_{\text{orbital}} = -0.051 \mu_B$  and  $M_{\text{spin}} = 0.018 \mu_B$ ). Considering the idealized high-symmetry environment of the  $[\text{UF}_6]^{2-}$  moiety, it is reasonable to explore the influence of vibronic effects on the magnetic properties of the complex. CASSCF results indicate that the  $A_{1g}$  ground state is separated from the excited states by more than  $1000 \text{ cm}^{-1}$  for both the crystal structure model and an idealized octahedral geometry. Thus, there is no ground state degeneracy and vibronic effects

must be related to a pseudo-Jahn-Teller mechanism.<sup>[22]</sup> To evaluate if vibronic coupling impacts the magnetic moments, a Hamiltonian was built with diagonal elements corresponding to state energies including spin-orbit effects (quasi-degenerate perturbation theory, QDPT) and a Zeeman term. The state interaction between the ground state, 0, and an excited state,  $a$ , is represented by the expression:

$$\mathcal{H}_{0a} = -\mu_B \mu_0 (\mathbf{g}_e \mathbf{S}_{0a} + \mathbf{L}_{0a}) \cdot \mathbf{H} + F_{0a} \lambda$$

where  $\mathbf{S}_{0a,i} = \langle \Psi_a | \hat{S}_i | \Psi_0 \rangle$  and  $\mathbf{L}_{0a,i} = \langle \Psi_a | \hat{L}_i | \Psi_0 \rangle$  for  $i = x, y$  and  $z$ . The first term corresponds to the Zeeman interaction and the second is the linear vibronic contribution with coupling constants:

$$F_{0a} = \left\langle \Psi_a \left| \frac{d\mathcal{H}_0}{dQ} \right| \Psi_0 \right\rangle$$

where  $\mathcal{H}$  is the QDPT Hamiltonian evaluated at the crystallographic geometry,  $\Psi_0$  and  $\Psi_a$  are ground state and excited state wave functions, respectively. Vibronic state interaction between excited levels was omitted from this treatment since many excited states are degenerate at the reference geometry. A model accounting for this interaction would require an explicit description of the active normal modes mixing each degenerate manifold. As the present interest focuses on the ground state magnetic moment, it is not necessary to include these terms. To estimate  $F$ , CASSCF calculations were performed at slightly displaced geometries and matrix elements were obtained by numerical differentiation (See [Supporting Information](#) for further details). The geometry was distorted towards the perfect octahedron. Vibronic mixing quickly increases the magnetic moment and then stabilizes for low displacement values (ca.  $0.05 a_0$ ;  $a_0$  is the Bohr radius unit; [Figure S4](#)). If we consider  $\lambda = 0.06 a_0$  as a representative displacement, we obtain  $M_{\text{orbital}} = 0.48 \mu_B$ , and  $M_{\text{spin}} = -0.26 \mu_B$ , which are in reasonable agreement with the experiment and point to a vibronic mechanism to justify the  $M_{\text{orbital}}$  and  $M_{\text{spin}}$  values.

To conclude, this work reports on the  $[\text{UF}_6]^{2-}$  complex, which is the first example of a structurally characterized hexafluorido actinide(IV) complex. Despite of the very weak magnetic moment of  $[\text{UF}_6]^{2-}$ , the detailed study and analysis of its magnetic properties combining state-of-the-art X-ray absorption spectroscopy, magnetometry and quantum chemical calculations have demonstrated the existence of relatively large spin and orbital magnetic moments. These moments are roughly one hundred times larger than those found in related  $5d$  systems with electronic singlet ground states.<sup>[23]</sup> These significant spin and orbital components should be considered in the future analyses of the magnetic exchange interactions in uranium(IV)-based materials and fuel the curiosity for a fundamental understanding of the electronic structure and magnetism of other actinide-containing molecules.

## Acknowledgements

K.S.P. and R.C. thank the Danish Research Council for Independent Research for a DFF-Sapere Aude Research Talent grant (4090-00201), the University of Bordeaux, the Region Nouvelle Aquitaine, the CNRS, the GdR MCM-2 and the MOLSPIN COST action CA15128. R.C. and J.R.L. are grateful to the France-Berkeley Fund and the CNRS (PICS N°06485) for funding. Research at the University of California, Berkeley was

supported by NSF Grant CHE-1800252 to J.R.L. D.A. thanks FONDECYT Regular 1170524 project for financial support. Powered@NLHPC: This research was partially supported by the supercomputing infrastructure of the NLHPC (ECM-02). M.A. and E.R. thank Ministerio de Economía y Competitividad for grant PGC2018-093863-B-C21 and for computacional resources to CSUC. M.A. acknowledges the Ministerio de Educación y Formación Profesional for an FPU predoctoral grant. E.R. thanks Generalitat de Catalunya for an ICREA Academia grant. The X-ray spectroscopy experiments were performed at the European Synchrotron Radiation Facility (ESRF, Grenoble, France).

PGC2018-093863-B-C21

## Conflict of interest

The authors declare no conflict of interest.

**Keywords:** uranium • fluorides • actinides  
• X-ray spectroscopy • magnetic properties • electronic structure

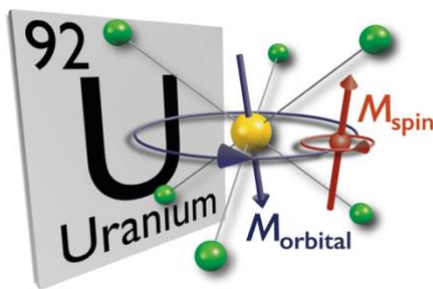
- [1] S. T. Liddle, *Angew. Chem. Int. Ed.* **2015**, *15*, 8604.
- [2] (a) J. D. Rinehart, J. R. Long, *J. Am. Chem. Soc.* **2009**, *131*, 12558; (b) J. D. Rinehart, K. R. Meihaus, J. R. Long, *J. Am. Chem. Soc.* **2010**, *132*, 7572; (c) D. P. Mills, F. Moro, J. McMaster, J. van Slageren, W. Lewis, A. J. Blake, S. T. Liddle, *Nat. Chem.* **2011**, *3*, 454; (d) F. Moro, D. Mills, S. T. Liddle, J. van Slageren, *Angew. Chem. Int. Ed.* **2013**, *52*, 3430; (e) K. R. Meihaus, S. G. Minasian, W. W. Lukens, S. A. Kozimor, D. K. Shuh, T. Tylliszczak, J. R. Long, *J. Am. Chem. Soc.* **2014**, *136*, 6056; (f) K. R. Meihaus, J. R. Long, *J. Am. Chem. Soc.* **2015**, *44*, 2517; (g) D. M. King, F. Tuna, J. McMaster, W. Lewis, A. J. Blake, E. J. L. McInnes, S. T. Liddle, *Angew. Chem. Int. Ed.* **2013**, *52*, 4921.
- [3] M. A. Antunes, J. T. Coutinho, I. C. Santos, J. Marcalo, M. Almeida, J. J. Baldovi, L. C. J. Pereira, A. Gaita-Arino, E. Coronado, *Chem. Eur. J.* **2015**, *21*, 17817.
- [4] (a) V. Mougél, L. Chatelain, J. Pecaut, R. Caciuffo, E. Colineau, J.-C. Griveau, M. Mazzanti, *Nat. Chem.* **2012**, *4*, 1101; (b) (f) V. Mougél, L. Chatelain, J. Hermle, R. Caciuffo, E. Colineau, F. Tuna, N. Magnani, A. De Geyer, J. Pecaut, M. Mazzanti, *Angew. Chem. Int. Ed.* **2014**, *53*, 819; (c) L. Chatelain, J. P. S. Walsh, J. Pécaut, F. Tuna, M. Mazzanti, *Angew. Chem. Int. Ed.* **2014**, *53*, 13434.
- [5] (a) A. Formanuik, A.-M. Ariciu, F. Ortu, R. Beekmeyer, A. Kerridge, F. Tuna, E. J. L. McInnes, D. P. Mills, *Nat. Chem.* **2017**, *9*, 578; (b) D. M. King, P. A. Cleaves, A. J. Wooles, B. M. Gardner, N. F. Chilton, F. Tuna, W. Lewis, E. J. L. McInnes, S. T. Liddle, *Nat. Commun.* **2016**, *7*, 13773; (c) M. Gregson, E. Lu, D. P. Mills, F. Tuna, E. J. L. McInnes, C. Hennig, A. C. Scheinost, J. McMaster, W. Lewis, A. J. Blake, A. Kerridge, S. T. Liddle, *Nat. Commun.* **2017**, *8*, 14137. (d) A. Bronova, T. Droß, R. Glaum, H. Lueken, M. Speldrich, W. Urland, *Inorg. Chem.* **2016**, *55*, 6848.
- [6] G. van der Laan, A. I. Figueroa, *Coord. Chem. Rev.* **2014**, *277-278*, 95.
- [7] (a) S. P. Collins, D. Laundry, C. C. Tang, G. van der Laan, *J. Phys.: Condens. Matter* **1995**, *7*, 9325; (b) P. Dalmas de Reotier, J. P. Sanchez, A. Yaouanc, M. Finazzi, Ph. Sainctavit, P. Krill, J. P. Kappler, J. Goedkoop, J. Goulon, C. Goulon-Gibbet, A. Rogalev, O. Vogt, *J. Phys. Condens. Matter* **1997**, *9*, 3291; (c) F. Wilhelm, N. Jaouen, A. Rogalev, W. G. Stirling, R. Springell, S. W. Zochowski, A. M. Beesley, S. D. Brown, M. F. Thomas, G. H. Lander, S. Langridge, R. C. C. Ward, M. R. Wells, *Phys. Rev. B* **2007**, *76*, 024425; (d) N. Magnani, R. Caciuffo, F. Wilhelm, E. Colineau, R. Eloirdi, J.-C. Griveau, J. Ruzs, P. M. Oppeneer, A. Rogalev, G. H. Lander, *Phys. Rev. Lett.* **2015**, *114*, 097203; (e) N. Magnani, R. Eloirdi, F. Wilhelm, E. Colineau, J. C. Griveau, A. B. Shick, G. H. Lander, A. Rogalev, R. Caciuffo, *Phys. Rev. Lett.* **2017**, *119*, 157204; (f) F. Wilhelm, J. P. Sanchez, J. P. Brison, D. Aoki, A. B. Shick, A. Rogalev, *Phys. Rev. B* **2017**, *95*, 235147.
- [8] (a) J. L. Ryan, J. M. Cleveland, G. H. Bryan, *Inorg. Chem.* **1974**, *13*, 214; (b) D. Brown, B. Whittaker, N. Edelstein, *Inorg. Chem.* **1974**, *13*, 1805; (c) B. Ordejón, L. Seijo, Z. Barandiarán, *J. Chem. Phys.* **2005**, *123*, 204502; (d) B. Ordejón, M. Korbowski, L. Seijo, Z. Barandiarán, *J. Chem. Phys.* **2006**, *125*, 074511.
- [9] a) Y.-L. Lai, R.-K. Chiang, K.-H. Lii, S.-L. Wang, *Chem. Mater.* **2008**, *20*, 523; (b) R. J. Francis, P. S. Halasyamani, J. S.; Bee, D. O'Hare, *J. Am. Chem. Soc.* **1999**, *121*, 1609; (c) B. Scheibe, S. Lippert, S. S. Rudel, M. R. Buchner, O. Burghaus, C. Peitzonka, M. Koch, A. J. Karttunen, F. Kraus, *Chem. Eur. J.* **2016**, *22*, 12145.
- [10] (a) M. P. Eastman, P. G. Eller, G. W. Halstead, *J. Inorg. Nucl. Chem.* **1981**, *43*, 2839; (b) J. H. Levy, J. C. Taylor, P. W. Wilson, *J. Chem. Soc. Dalton Trans.* **1976**, 219.
- [11] (a) R. K. Thomson, C. R. Graves, B. L. Scott, J. L.; Kiplinger, *Dalton Trans.* **2010**, *39*, 6826; (b) R. R. Ryan, R. A. Penneman, B. Kanellakopoulos, *J. Am. Chem. Soc.* **1975**, *97*, 4258.
- [12] D. R. Kindra, W. J. Evans, *Chem. Rev.* **2014**, *114*, 8865.
- [13] (a) A. Yaouanc, P. Dalmas de Réotier, G. van der Laan, A. Hiess, J. Goulon, C. Neumann, P. Lejay, N. Sato, *Phys. Rev. B* **1998**, *58*, 8793; (b) P. Dalmas de Réotier, A. Yaouanc, G. van der Laan, N. Kerna-vanois, J.-P. Sanchez, J. L. Smith, A. Hiess, A. Huxley, A. Rogalev, *Phys. Rev. B* **1999**, *60*, 10606; (c) V. N. Antonov, B. N. Harmon, A. N. Yaresko, *Phys. Rev. B* **2003**, *68*, 214424; (d) A. N. Yaresko, V. N. Antonov, B. N. Harmon, *Phys. Rev. B* **2003**, *68*, 214426.
- [14] Thole B.T., van der Laan G. *Phys. Rev. A.* **1988**, *38*, 1943.
- [15] M. Finazzi, Ph. Sainctavit, A.-M. Dias, J.-P. Kappler, G. Krill, J.-P. Sanchez, P. Dalmas de Réotier, A. Yaouanc, A. Rogalev, J. Goulon, *Phys. Rev. B* **1997**, *55*, 3010.
- [16] G. van der Laan, B. T. Thole, *Phys. Rev. B* **1996**, *53*, 14458.
- [17] M. Colella, G. R. Lumpkin, Z. Zhang, E. C. Buck, K. L. Smith, *Phys. Chem. Minerals* **2005**, *32*, 52.
- [18] P. Carra, B. T. Thole, M. Altarelli, X. Wang, *Phys. Rev. Lett.* **1993**, *70*, 694.
- [19] B. T. Thole, P. Carra, F. Sette, G. van der Laan, *Phys. Rev. Lett.* **1992**, *68*, 1943.
- [20] P.-Å. Malmqvist, B. O. Roos, *Chem. Phys. Lett.* **1989**, *155*, 189.
- [21] (a) C. Angeli, R. Cimraglia, S. Evangelisti, T. Leininger, J.-P. Malrieu, *J. Chem. Phys.* **2001**, *114*, 10252; (b) C. Angeli, R. Cimraglia, J.-P. Malrieu, *Chem. Phys. Lett.* **2001**, *350*, 297.
- [22] (a) I. B. Bersuker, *Chem. Rev.* **2013**, *113*, 1351; (b) I. B. Bersuker, *Chem. Rev.* **2001**, *101*, 1067.
- [23] K. S. Pedersen, D. N. Woodruff, S. K. Singh, A. Tressaud, E. Durand, M. Atanasov, P. Perlepe, K. Ollefs, F. Wilhelm, C. Mathonière, F. Neese, A. Rogalev, J. Bendix, R. Clérac, R. *Chem. Eur. J.* **2017**, *23*, 11244.

---

## COMMUNICATION

---

The electronic ground state of the weakly magnetic U(IV) was studied in great details for the simple, structurally characterized,  $[\text{UF}_6]_2^{2-}$  anion combining X-ray absorption spectroscopy, magnetometry and quantum chemical calculations. The decomposition and quantification of the relatively large spin and orbital magnetic moments provide key information for an improved understanding of the complex electronic structures of actinide ions.



*Kasper S. Pedersen,\*  
Katie R. Meihaus, Andrei Rogalev,\*  
Fabrice Wilhelm, Daniel Aravena,  
Martín Amoza, Eliseo Ruiz,  
Jeffrey R. Long, Jesper Bendix and  
Rodolphe Clérac\**

**$[\text{UF}_6]_2^{2-}$ : A Molecular Hexafluorido Actinide(IV) Complex with Compensating Spin and Orbital Magnetic Moments**